Covid-19 Epidemic Dynamic Including Barriers of Circulation

Sebastião C. P. Gomes and Igor O. Monteiro

Federal University of Rio Grande (FURG), Mathematics, Statistics and Physics Institute

Rio Grande, Brazil, sebastiaogomes@furg.br, igor.monteiro@furg.br

Abstract: In this article we analyze the evolutionary dynamics of the novel coronavirus epidemic (covid-19) using observed data from several cities and places in the world. We have used a SIR-type (Susceptible, Infectious and Recovered) model improved with some adaptions in order to increase its predictive skills, i.e., we have included the circulation restriction effect and considered a phenomenon we have called adherence zone, generating the Modified SIR model (ModSIR). Comparing the results produced with ModSIR with real observations obtained for several places in the world we have found that ModSIR presented good predictive skill, as long as combined with good enough parametric identification. At the end of this article we present a study in which we simulated an epidemic in a hypothetical city of 211000 inhabitants. We have extracted several useful conclusions by analyzing some epidemic scenarios in which we evaluate epidemic control by adopting the circulation restriction as a control variable.

Keywords: Epidemics, coronavirus, dynamic model, ModSIR model.

1. Introduction

The epidemic caused by the novel coronavirus surprised by its fast spread and high contagiousness in humans. Despite of being recent, several related articles and technical notes have been published recently. Interesting contagion rates based on China epidemic has been published by Li *et al.* [1]. Several studies use compartmental models and its variations: SIR (Susceptible, Infectious and Recovered) and SEIR (Susceptible, Exposed, Infectious and Recovered), the latter being more used. Hamzah*et al.* [2] used the SEIR model without consider quarantine or circulation restriction. They did not compared their model estimates with real observations but presented an up to date revision on the subject. In [3] real time mobility data were used in order to monitor efficiency and impact of preventive actions adopted in Chinese provinces. Amire and Torres [4] used the SEIR model to analyze the Ebola virus epidemic in Liberia, Africa. In [5] the SEIR model was applied in order to predict the epidemic evolution in the city of Belo Horizonte, Brazil. Important parameters of novel coronavirus epidemic have been obtained by specific medicine studies [6]. In [7] a study using the SEIR model applied to novel coronavirus epidemic in the city of Wuhan, China, is presented in which the epidemic growth responses to different model parameter choices were analyzed. Hubbs [8] also applied the SEIR model in order to analyze epidemic peak responses to different parameter choices. In Quintans and Silva [9] the HIV and flu epidemics were studied including model stability analyzes. Vast bibliography on epidemic modelling can be found in form of articles and theses. An interesting study is performed by Kabir *et al.* [10] in which they used the SIR model to evaluate the population awareness effect on the epidemic growth. The fear factor due to the disease was incorporated in the SIR model by Epstein *et al.* [11]. Zhou et al. [12] developed studies on stability analysis of a discrete multigroup SIR model. Song et al. [13] also introduced stability Lyapunov analysis in a SIR model with distributed delays and nonlinear incidence rate. Londoño [14] presents some parameter estimation methods developed to SIR and SEIR models. He was particularly interested in the basic reproduction number R_0, which constitutes the main parameter related to the contagion speed. The SIR model in its discrete formulation is largely discussed by Sabeti [15] where he includes the population age structure effect on the epidemic. Zhen et al. [16] propose modifications in a SIR model to incorporate Laplacian diffusion and spatiotemporal delay to model the transmission of communicable diseases. In Dorn [17] different Dengue fever epidemics were compared based on its basic reproduction number. An extensive number of epidemic modeling studies can be also found in bibliographic references presented in above mentioned articles and theses.

In this study we apply the SIR model in order to investigate the novel coronavirus epidemic evolution. Our approach uses the simple SIR epidemic model due to the difficult task of parameters estimation which is necessary in more complex models [6]. Increasing model complexity leads to the need of more parameters to be estimated that, in turn, increases the parametric uncertainties. However, despite of the simplicity involved in SIR model formulation, we have made two significant modifications generating ModSIR model, with the purpose to improve its predictability which made it able to reproduce the observed data. The first modification introduced is related to make the model able to represent the social isolation of part of the population. The second one consists in the representation of an effect that we have called adherence in that the epidemic evolution is interrupted when a set of necessary conditions are satisfied and the basic reproduction number is close to 1. These two new proposals increase the model ability to reproduce real observed data. To sum up, in spite of choose a more complex model we have opted to choose a simpler model (SIR), with few parameters, and adapt it in order to improve its predictive skills, generating ModSIR model.

2. Dynamic Model

In this section we intent to present the SIR model in its original formulation as well as presenting the modifications that we have proposed to generate ModSIR. The purpose is to make the model more predictive mainly including circulation restriction effects and the adherence dynamic phenomena.

2.1 The ModSIR model

The SIR model was originally formulated by Kermack and McKerndric in 1927 [10]. Figure 1 presents a block diagram with its three compartments.

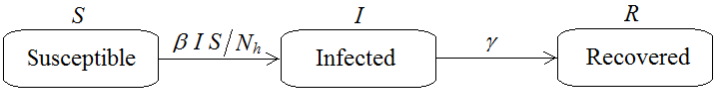

Figure 1. Block diagram representing the three SIR model compartments.

In SIR model S represents the number of susceptible individuals which are available to suffer virus infection. I represents the number of infected individuals and R represents the number of recovered individuals. N_h corresponds the number of total inhabitants that in our study is $N_h = S + I + R$, where we are ignoring new births and natural deaths. Choosing this simple SIR model we need only to know two external parameters: β (the infection growth rate) and γ (the recover rate). Thus in SIR modeling the epidemic is governed by the following set of ordinary differential equations:

$$\begin{aligned} \dot{S} &= -\frac{\beta SI}{N_h} \\ \dot{I} &= \frac{\beta SI}{N_h} - \gamma I \\ \dot{R} &= \gamma I \end{aligned} \tag{1}$$

We have made two modifications in the above mentioned SIR model in order to make it more predictive and adapted to the novel coronavirus epidemic. We named it Modified SIR model (ModSIR). The first one was to include a dynamical effect that we have called adherence zone. As will be explained in the next section, the adherence zone enables ModSIR to capture the dynamics in the case of some predefined conditions being reached, causing the number of infected individuals goes quickly to zero. Another original modification we are adopting consists in determining the infection growth rate (β) as function of the circulation percentage (p). We have defined the circulation percentage p as being the parcel of the population which is tolerated to freely circulate divided by the total number of inhabitants.

Thus, p is permitted to vary in the interval $0 \leq p \leq 1$. With this modifications, ModSIR model have the following formulation:

$$\dot{S} = -\frac{\beta(p)SI}{N_h}$$

$$\dot{I} = \frac{\beta(p)SI}{N_h} - \gamma I \tag{2}$$

$$\dot{R} = \gamma I$$

2.2 Infection growth rate determination

Each epidemic affecting the humanity has its own parameters and specific control variables. In the case of the novel coronavirus, the circulation percentage (p) has showed being the main control variable worldwide. Consequently, it is fundamental to consider this effect in any dynamic model aiming to represent the novel coronavirus epidemic dynamics. The first step is to identify the novel coronavirus natural parameters β and γ without consider any circulation restriction. The γ parameter is not affected by the circulation restriction effect being constant and is related to the infection time T_{inf} by $\gamma = 1/T_{inf}$. In our study we have adopted the value $T_{inf} = 5.5$ *days* which has been identified in the Hubei epidemics [13] and gives $\gamma = 0.1818$. We have also used the β parameter estimated in [13] which corresponds to $R_0 = 2.25$ and $\beta_0 = \gamma R_0 = 0.4091$. Because we have considered the effect of circulation restriction on the β parameter in our study, we have set $\beta(p = 1) = \beta_0 = 0.4091$, i.e., β_0 is our β when any circulation restriction is adopted. We remind here that R_0 is the basic reproduction number which is related to the contamination speed. A high R_0 number implies in a fast contamination speed.

Initially we performed some simulations with the purpose to validate the adopted β_0 and γ values. In Figure 2a the results obtained with SIR model are compared to observations in the province of Hubei, China for the first 20 days. We see that in fact initially the parameters β_0 and γ enable the model to reproduce the observed data. However, subsequently the government starts to impose restrictions in which only a population parcel can freely circulate. In practice, because the area of the city remains the same, the effect of the circulation restriction is to decrease the spatial density of individuals susceptible to the virus which, in turn, results in the decrease of the growth infection rate β as one can clearly see observing the Hubei epidemic evolution in Figure 2b. In Hubei important circulation restriction was imposed resulting in effective epidemic control. Figure 2b shows a comparison of the accumulated cases between the real observed data and model results. We can see that SIR model performed well in this simulation. It is important to say that in order to reproduce the observed data we had to adopt different values for the infection growth rate β namely $\beta = 0.63\gamma R_0$ $(15 < t \leq 20)$; $\beta = 0.6\gamma R_0$ $(20 < t \leq 22.5)$; $\beta = 0.56\gamma R_0$ $(22.5 < t \leq 25)$ and $\beta = 0.16\gamma R_0$ $(t > 25)$. This β values were obtained by trial and error aiming to the best fit between model results and observed data. An important inference of this variation in the β parameter is that the circulation restriction was step by step being intensified until twenty-fifth day when a drastic limitation was adopted causing the epidemic interruption (the number of infected in Figure 2b goes to zero and the accumulated cases become henceforth constant). We remark that this is the ideal case to be followed when the health system is close to the collapse. Thus we started to look for a function $\beta(p)$ that relates the infection growth rate β with the circulation percentage p.

With the aim to find the relation $\beta(p)$ we performed an experiment where we considered a hypothetical city of $N_h = 211000$ inhabitants (population of Rio Grande, Brazil). Then, several simulations (Figure 3a) were accomplished with the SIR model presented in the set of equations (1) where we adopted the parameters β_0 and γ above described for the province of Hubei. The several simulations plotted in Figure 3a differ by the adopted number of inhabitants N_h. We have tested $N_h = \rho 211000$ varying ρ as: ρ=1, 0.85, 0.7, …., 0.1. The maximum values (end of the epidemic cycle) of the

accumulated cases in the different produced curves were stored in a file. Then, adopting $N_h = 211000$ inhabitants constant we did another experiment varying the β value until we have found for each ρ the respective $\beta(p = \rho)$ that produced the same stored final number of accumulated cases as in Figure 3a. The several curves produced when varying the β parameter are presented in Figure 3b with the correspondent circulation percentage p. We have also considered more three cases ($p = 0.04, 0.06$ and 0.08), which are not shown in Figure 3b due to scale.

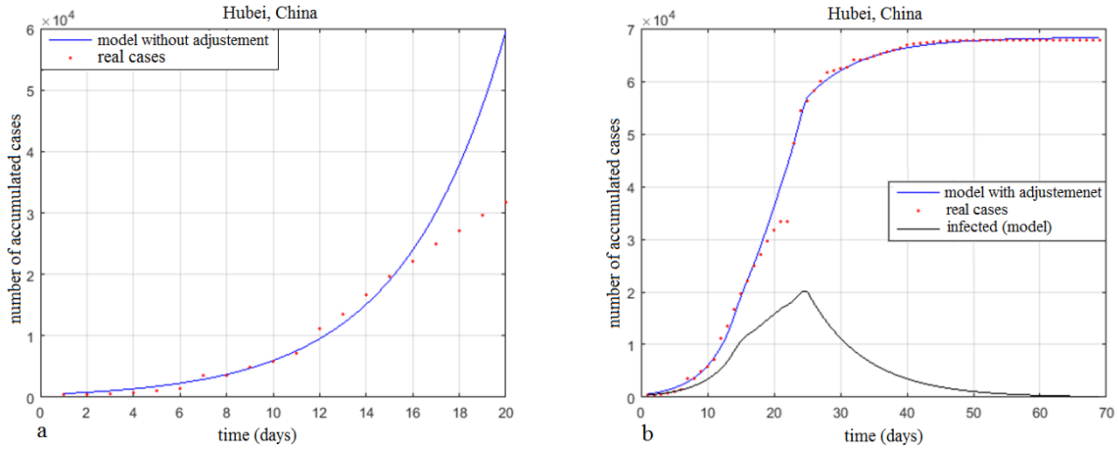

Figure 2. Imposed variations on β in order to simulate the same real data observed in Hubei: t>15 ($\beta = 0.63\beta_0$); t>20 ($\beta = 0.6\beta_0$); t>22.2 ($\beta = 0.56\beta_0$); t>25 ($\beta = 0.16\beta_0$); $\beta_0 = \gamma R_0$.

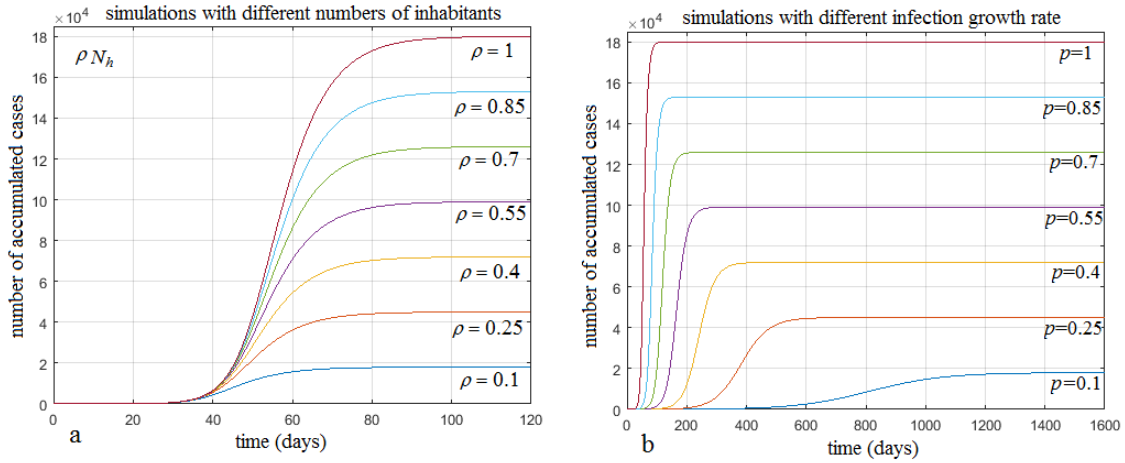

Figure 3.Simulations with variable population (3a) and with variable circulation percentage (3b).

We have identified values $\beta(p)$ for each curve in Figure 3b obtaining a total of ten points $[p_i, \beta(p_i)]$ that were fitted by seventh order polynomial:

$$\beta(p) = a_1 p^7 + a_2 p^6 + \cdots + a_7 p + a_8 \tag{3}$$

The polynomial in equation (3) is specific for the parameters: $T_{inf} = 5.5$ dias $\rightarrow \gamma = 0.1818$; $R_0 = 2.25$; $\beta_0 = \gamma R_0 = 0.4091$ obtained for Hubei, China. It can be normalized by $\beta_n(p) = \beta(p)/(\gamma R_0)$. Thus, an equivalent growth rate:

$$\bar{\beta}(p) = \beta_n(p)\bar{\gamma}\bar{R}_0 \tag{4}$$

can be applied to other cities and regions with different values for the parameters R_0 and γ. Figure 4 shows the growth rate curves as a function of the circulation percentage. We remark that, when circulation becomes smaller than 8%, the curves are adjusted by a quadratic function to quickly conduct its infection growth rate to zero. The region in which the circulation percentage is close to zero is what we

are calling the adherence zone. This region must exist when the circulation percentage is close to zero, i.e., when circulation restriction is almost complete the epidemic is interrupted and the infected number goes to zero stabilizing the accumulated number of infected cases which become constant (as we can see in Hubei data). However, it is difficult to know the exact circulation percentage limit (p_{lim}) in which the adherence zone becomes effective. In this study we have adopted the 8% value ($p_{lim} = 0.08$). The following algorithm is used to generate the growth rate:

$$\beta(p) = \frac{1}{\gamma R_0}(a_1 p^7 + a_2 p^6 + \cdots + a_7 p + a_8)\bar{\gamma}\bar{R}_0$$

$$\begin{aligned}
&if\ p \le p_{lim} \\
&\quad x_f = p_{lim};\ y_f = \beta(x_f);\ a = \beta'(x_f); \\
&\quad A = \begin{bmatrix} x_f^2 & x_f \\ 2x_f & 1 \end{bmatrix}; \vec{B} = \begin{pmatrix} y_f \\ a \end{pmatrix}; \\
&\quad \vec{\alpha} = A^{-1}\vec{B}; \\
&\quad \beta(p) = \alpha_1 p^2 + \alpha_2 p; \\
&end
\end{aligned} \tag{5}$$

It is noted that the adherence zone is an order 2 polynomial which cross the origin and has the same derivative of the seventh order polynomial at the point (x_f, y_f). This is an idealized curve: we know that the growth rate goes to zero when the circulation percentage tends to zero but the exact form of this curve is unknown. The exact percentage p_{lim} in which the adherence zone become active is also unknown but we have obtained good results with the value 8%. As initial test, we again simulate the Hubei epidemic, this time only varying the circulation percentage p and using $\beta(p)$ obtained by the algorithm (5). From this point on, all simulations are done with the ModSIR model (equations (2) and algorithm (5)). Figure (4) shows a comparison between the simulated and observed real data. On the right we present the values of the used circulation percentage p which gives a good fit between model results and observed real data. We have adopted that the transition between two p values is not abrupt but we forced it to follow a cubic spline from one step to the other as can be seen in the example in Figure 4 (right). It is natural to suppose this smooth curve in the transition of one step to the other because in practice the population parcel does not enter in social isolation immediately. We can note that the circulation restriction in Hubei was very severe attaining at end the value of 1.3% ($p = 0.013$).

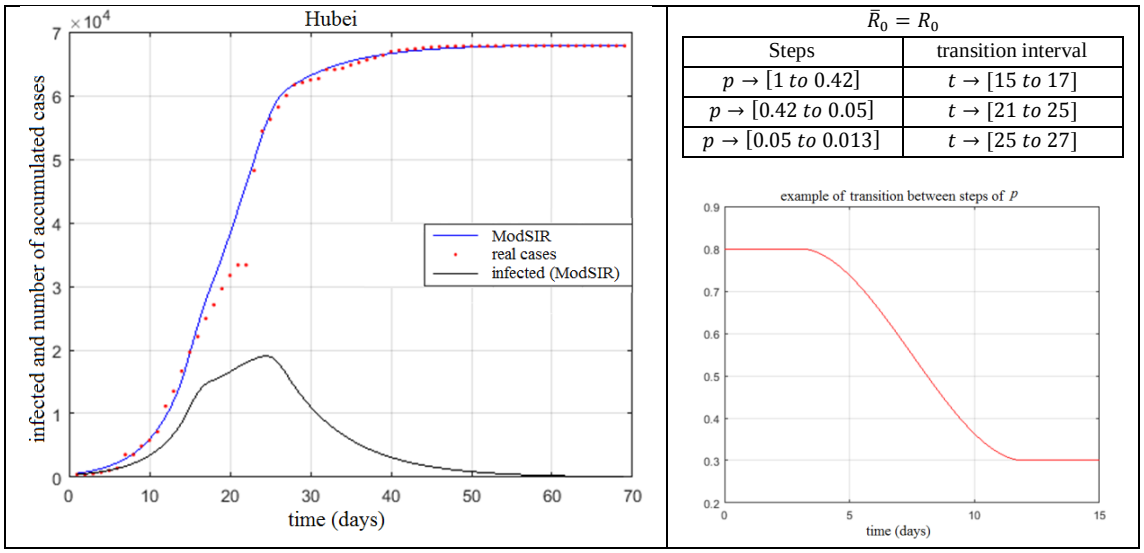

Figure 4. Epidemic control applied to Hubei, China: simulation with ModSIR and real data.

Figure 5a presents the growth rate $\beta(p)$ obtained with the proposed algorithm (5) and the original Hubei R_0. Figure 5b shows the resulting curves when different R_0 values are adopted. We observe that vertical displacements on the curve $\beta(p)$ are produced when the R_0 parameter was changed by an amount. Thus, an increase/decrease in the basic reproduction number produces an increase/decrease in the growth rate curve in the whole interval [0 1] of the circulation percentage (p).

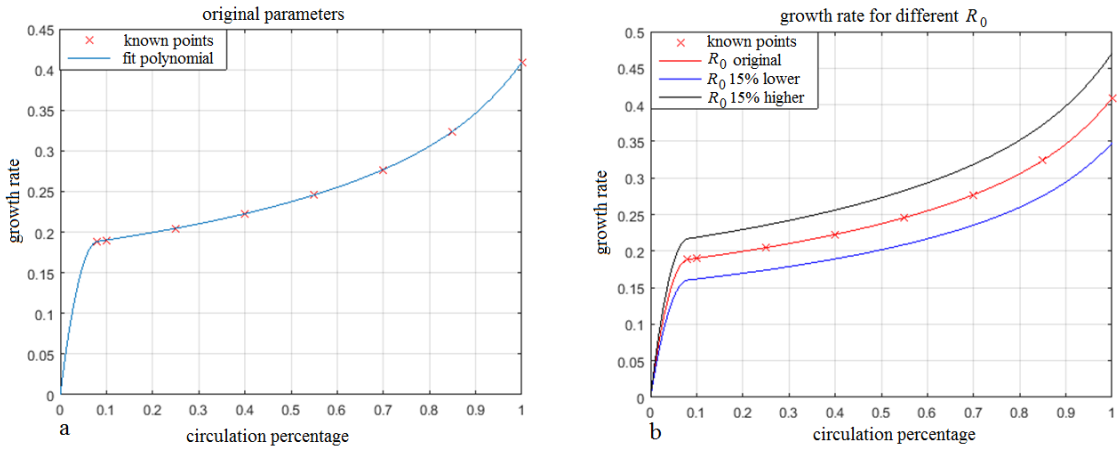

Figure 5. Curves: $\beta(p)$ with the original parameters (5a); $\beta(p)$ for different R_0 values (5b).

3. Confrontation Between Real Data and Simulation Results

In this section we will apply the generic function (algorithm (5)), which gives the infection growth rate as a function of the circulation percentage, for the purpose to simulate and analyze the epidemic evolution in other cities and regions. We remark that our modeling approach also permits the identification of the basic reproduction number R_0 of an specific region namely: starting from Hubei R_0, other simulations are made varying R_0 by an small amount until a good agreement between model results and observed real data is reached. This procedure must be applied only for the initial period of epidemics where there is still no circulation restriction actions imposed to the population. We have analyzed the following Spanish communities: Andaluzia, Murcia, Aragon, and Asturias. In addition to these Spanish communities we also have analyzed the cities of Madrid, Spain, and New York, USA. To the Spanish communities and Madrid it was considered the period between 02/20/2020 and 04/16/2020. The observed real data are presented by red dots in Figure 6, 7 and 8.

Results obtained for the Spanish communities and Madrid are presented in Figures 6 and 7, respectively. Figure captions also presents the identified basic reproduction number $\bar{R}_0$ for each case and the circulation restriction p, with the respective time intervals between two consecutives p steps. In Spain circulation restriction actions were only imposed in the twenty-fourth day after the first registered infected case which occurs on 02/20/2020. Observed data used spans from 02/20/2020 to 04/16/2020 (57 days). After 04/16/2020 we also present the ModSIR model prediction for the next days. Analyzing observed and model results we note the following remarks:

i) The basic reproduction number R_0 used in the other cities does not differ from the original Hubei R_0 by an amount greater than 15%;

ii) The variations in the circulation percentage p applied on each simulation were effective to produce a good agreement between observed real data and modeled curves, corroborating the predictive skill of the proposed model if its parameters are correctly set;

iii) We can observe for each case that the restrictions in people circulation were effective to prevent the epidemic increase;

iv) Particularly in Madrid case, a stronger restriction after day 57 would produce a stronger reduction in the number of infected individuals, as seen in Figure 7b.

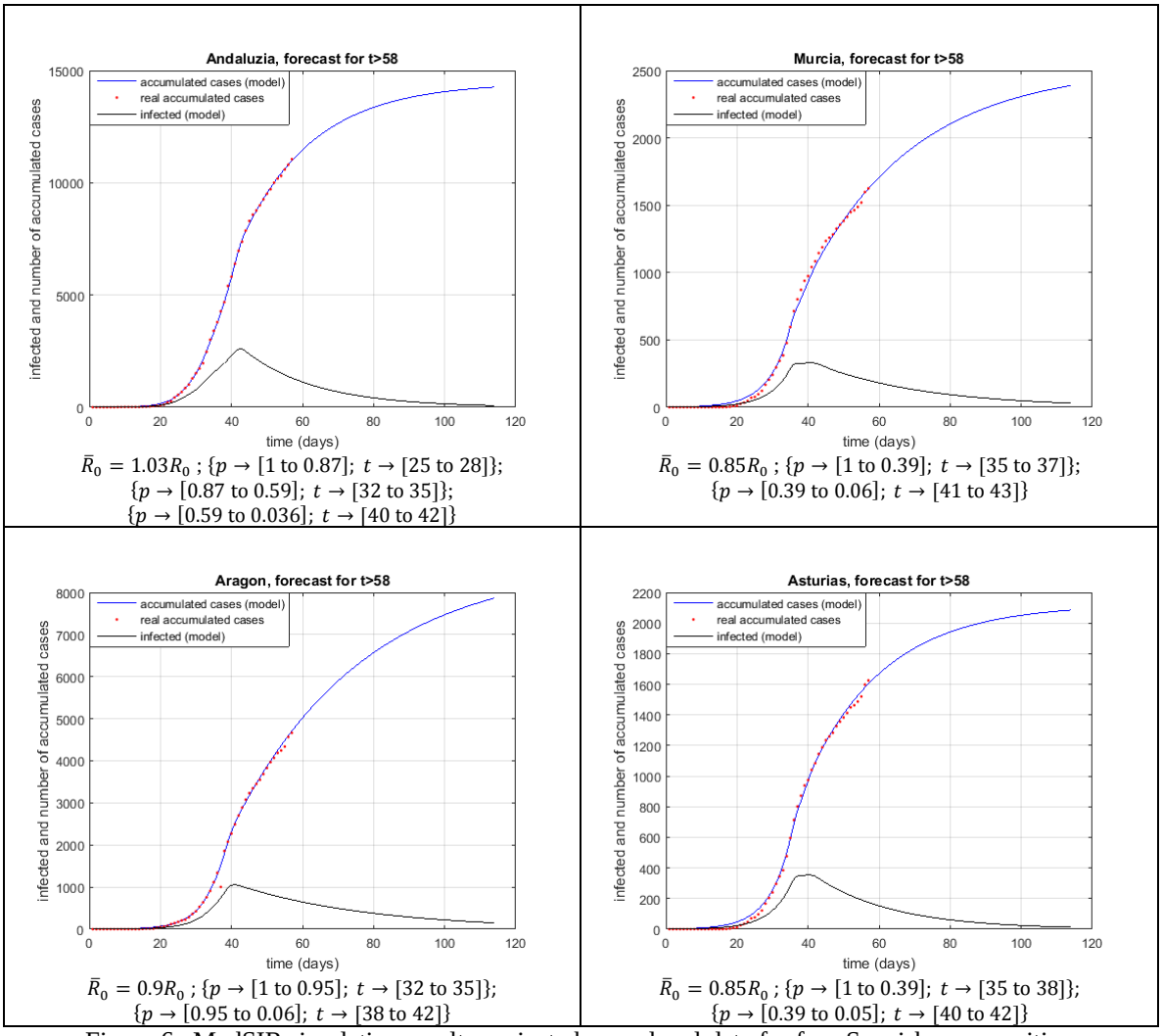

Figure 6. ModSIR simulation results against observed real data for four Spanish communities.

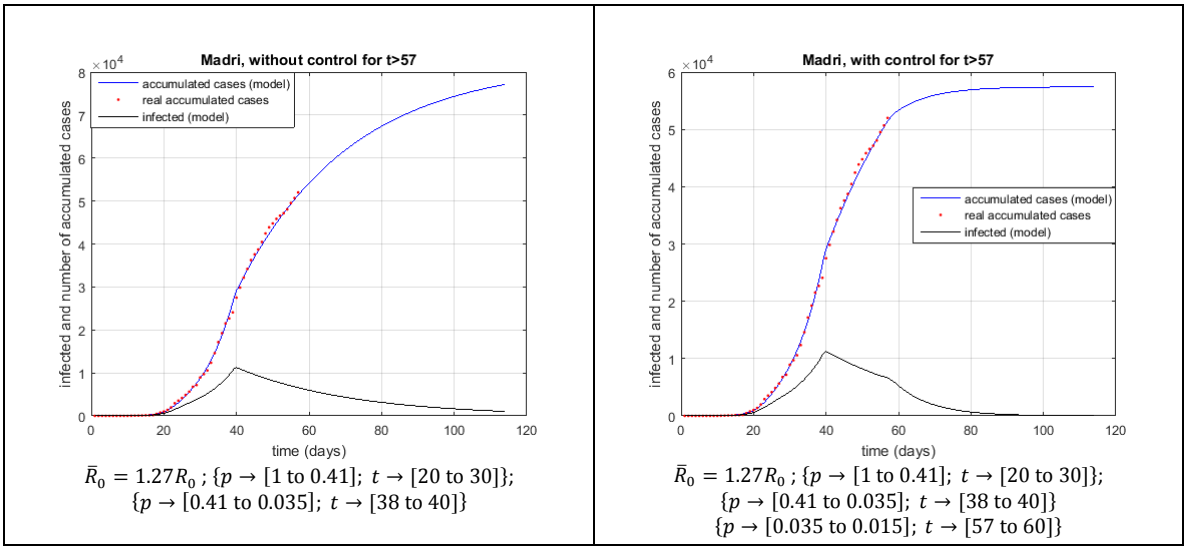

Figure 7. ModSIR simulations and observed real data for the city of Madrid with and without stronger restriction after day 57.

Figure 8 present results of simulated and observed real data for New York City. In this case observed real data start on 03/03/2020 after the first infected case and finish on 04/17/2020 spanning a period of 47 days. An important observation in the case of New York City is that its initial R_0 is 55% greater than that observed in Hubei. This fact is probably related to the high population density in this city but there are other causes as, for example, the great number of individuals that arrive in this city by its huge airports. As we did with Spain data, we also show ModSIR model prediction spanned for next days. On the left we see that the government actions to restrict circulation were still not totally effective to interrupt epidemics until day 47 although we can already see a line tendency in infection growth. We also simulate the epidemic evolution in New York City considering a stronger restriction after day 47, similar to that applied in Hubei. Results are presented on the right panel where we can see that in this case the number of infected goes quickly to zero presenting a response time similar to Hubei.

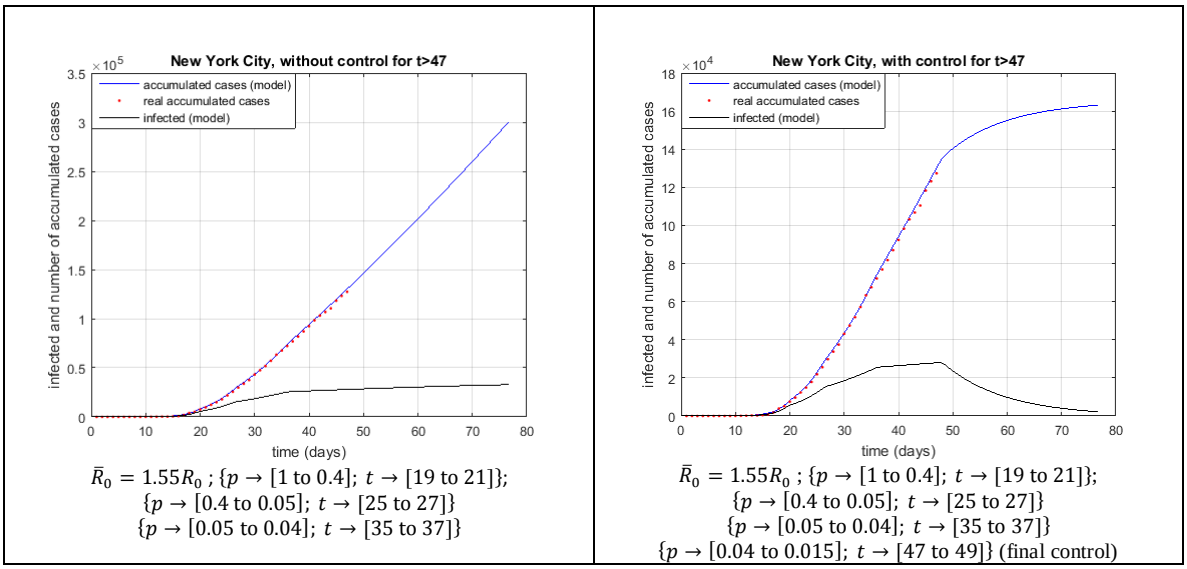

Figure 8. ModSIR simulations confronted with observed real data for New York City.

4. Simulations with Control

We have said that the main control variable worldwide in novel coronavirus epidemic has been the circulation percentage. Thus, in this section we aim to show how we could cause epidemics interruption by controlling the circulation percentage which is an available variable to the public administration. We have assumed a hypothetical city of 211000 inhabitants. We also considered the Hubei initial parameters namely $T_{inf} = 5.5$ dias $\to \gamma = 0.1818;\ R_0 = 2.25;\ \beta_0 = \gamma R_0 = 0.4091$. This parameters are used in algorithm (5) which gives us the infection growth rate as a function of the circulation percentage.

In Figure 9 we see several curves representing the number of infected individuals considering different circulation percentage values. We can see that the infected peak height decrease and it is displaced to right when the circulation percentage is decreased. This pattern has popularly been called the flattening curve effect.

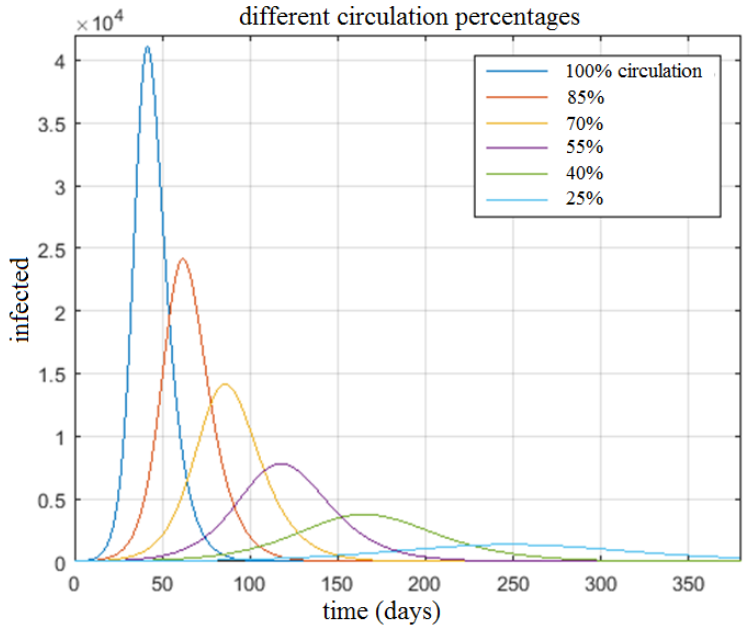

Figure 9. ModSIR Simulations considering several circulation percentage values.

Figure 10 highlights the adherence effect which can also be observed in the beginning of an epidemic process. We have intuitively supposed the adherence effect starts if the three conditions below happen simultaneously:

i) The number of accumulated cases $C = (I + R)$ during a time interval Δt_{lim} increase smaller than a predefined value C_{lim}, i.e., if $\frac{C_f - C_i}{\Delta t_{lim}} < C_{lim}$, with C_i and C_f representing the initial and final number of accumulated cases on the interval Δt_{lim};

ii) $R_0(p) = \frac{\beta(p)}{\gamma} < 1.05$;

iii) The number of infected individuals is smaller than a predefined limit: $I < I_{lim}$.

In our experiment involving a hypothetical city the adherence effect was observed when the circulation percentage attains a value smaller than 10% ($p \leq 0.1$). The limits adopted were $I_{lim} = 5$; $C_{lim} = 1$; $\Delta t_{lim} = 35$. When $p = 0.1$, we obtain $\beta(p) = 0.1903$ using algorithm (5) which gives $R_0(p) = 1.046$ (below the limit 1.05). In this case dynamics is "captured" when $t = 35$ *days*, finishing epidemics when the number of accumulated cases becomes constant. This dynamic capture occurs because when $p = 0.1$ (in this example) the adherence mode drives p through a cubic spline to be a small value (0.02). Thus $\beta(p)$ is forced to follow an adherence trajectory along a quadratic curve (as in Figure 5). We remark that the adherence mode occurs because in this example infection was in its beginning while the circulation percentage was small, equivalent to 10% ($p = 0.1$). It can occur in small cities which the accumulated cases in the first 35 or 40 days are not larger than 30 (for example) and, simultaneously, the circulation percentage is small, less than 10%. We believe this effect can be observed in practice although it can be very difficult to estimate with accuracy the true parameter values (which probably are also local dependent).

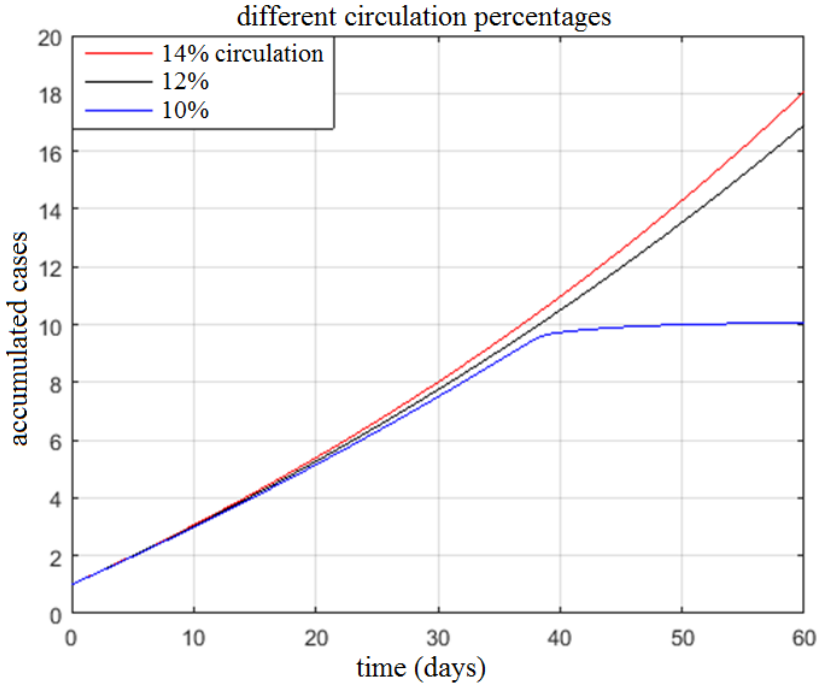

Figure 10. ModSIR Simulation illustrating the adherence phenomenon.

In Figure 11 we present an example of epidemic control by circulation restriction starting from $t = 25$ *days*. In this example we considered that the hypothetical city is with a circulation restricton percentage of $p = 0.65$ which does not prevent the increase in the infected number. We remark that several cities in our country (Brazil) are now with this weak level of restriction. After $t = 25$ *days* we force a strong level of restriction imposing $p = 0.015$, i.e., only 1.5% of individuals are allowed to circulate freely. Figure 11 shows that this control was effective to reduce quickly the number of infected and stabilizing the number of accumulated cases in 600. Comparing with the Hubei case presented in Figure 4 we see a similar pattern with about the same attenuation time.

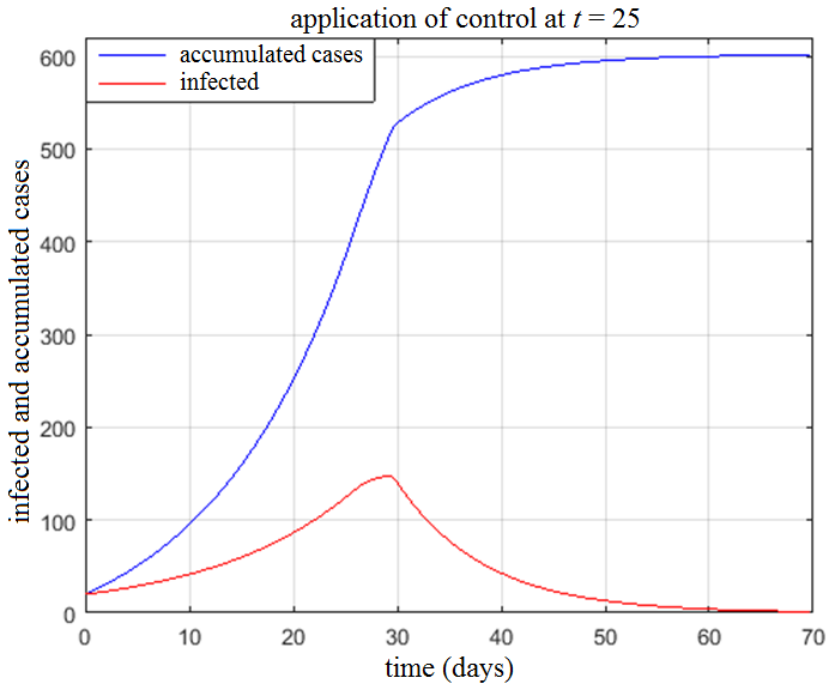

Figure 11. Simulation with application of a control by restricting circulation after $t = 25$ *days* (p was 0.65 and become 0.015 during $\Delta t = 5$ *days*).

In Figure 12 is presented the so-called second wave of infected which can occur if circulation restrictions are weakened before the ideal time. In this example a control equal to that presented in Figure 11 is applied in $t = 25\ days$ (first infection peak) reducing quickly the number of infected individuals. Then, before the ideal time (65 days in this case), we simulate a restriction weakening in $t = 45\ days$ by increasing p from 0.015 to 0.8 (80% of population return to freely circulate). As result we see a new increase in infected number producing a second wave of infected individuals. When t was 85 days we imposed a new effective circulation restriction that definitely interrupt epidemics.

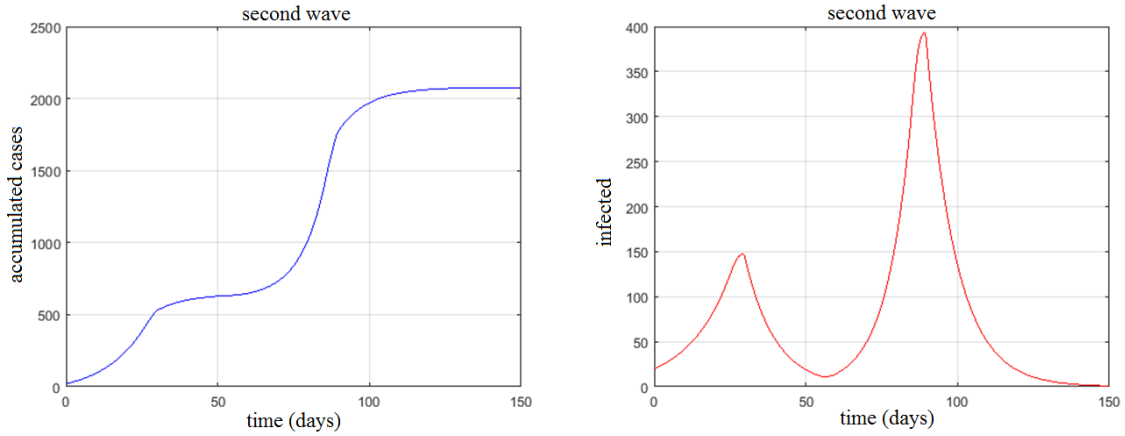

Figure 12. Simulation illustrating the danger of prematurely weakening circulation restriction before the ideal time being reached: $p = 0.65$ in $(t \leq 25\ days)$; $p = 0.015$ in $(25 < t \leq 55\ days)$; $p = 0.8$ in $(55 < t \leq 85\ days)$; $p = 0.015$ in $(t > 85\ days)$.

5. Conclusions

The study presented here was accomplished using observed real data from several places and cities which are not detailed because of space restrictions. It is well-known that the novel coronavirus epidemic data are significantly underestimated imposing the need of caution in its use and selection. Despite that the Hubei data seems to be a very interesting data set because it presents a complete cycle of novel coronavirus infection including an effective epidemic control.

In this study we followed the strategy of adopting a simpler model in which the number of parameters is small, reducing the parametric uncertainties. We have used the SIR model that is the simplest structure between the available compartmental epidemic models. However we implement some modifications to develop ModSIR model which improves its predictability as we had seen by comparison with observed real data. We initially note that the infection growth rate was variable over time in observed real data and this variation was related to the government actions imposing circulation restrictions. We saw that decreasing the circulation percentage induces a decrease in the infection growth rate parameter. Thus we investigate and establish a function as an algorithm that relates the circulation percentage with the infection growth rate. Another improvement we have applied to ModSIR model was an adherence zone which drives epidemic when some predefined conditions occur simultaneously (being the most important predefined condition a basic reproduction number close to 1). After applying these modifications, several simulations were made in which we have observed a good agreement with observed real data. The proposed model enables us to simulate other scenarios where we tested epidemic control by restricting people circulation. We have verified that ModSIR model performed well despite of its very limited number of parameter when compared with more complex epidemic models. Thus, we have showed that for the case of the novel coronavirus epidemics a simpler model with some clever adaptions can significant improve the model skills enabling it to reproduce the observed real data. In a future study we intend to deep our method of epidemic control by applying nonlinear control techniques.

References

1. Ruiyun Li, Sen Pei, Bin Chen, Yimeng Song, Tao Zhang, Wan Yang, Jeffrey Shaman. Substantial undocumented infection facilitates the rapid dissemination of novel coronavirus (SARS-CoV2). Science, DOI:10.1126/science.abb3221, (2020).
2. Binti Hamzah F A, Lau C, Nazri H, Ligot D V, Lee G, Tan CL, et al. Corona Tracker: Worldwide COVID-19 Outbreak Data Analysis and Prediction. [Submitted]. Bull World Health Organ. E-pub: 19 March 2020. doi: 10.2471/BLT.20.255695.
3. Moritz U. G. Kraemer, Chia-Hung Yang, Bernardo Gutierrez, Chieh-Hsi Wu, Brennan Klein, David M. Pigott. The effect of human mobility and control measures on the COVID-19 epidemic in China. Science, Mar, 2020, doi: 10.1126/science.abb4218.
4. Amira Rachah, Delfim F. M. Torres. Analysis, simulation and optimal control of a SEIR model for Ebola virus with demographic effects. DOI: 10.1501/Commua1_0000000841. Preprint of a paper whose final and definite form is with Commun. Fac. Sci.Univ. Ank.Ser. A1 Math. Stat., ISSN: 1303-5991. Article accepted for publication 01 May2017.
5. Alexandre C. L. Almeida et al. Analysis of the effect of measures to contain the spread of COVID-19 in Belo Horizonte. Technical report. March, 2020. https://ufmg.br/storage/2/5/a/7/25a7163c7fb5575ab6d81b5a05bfd844_15863100172762_298779967.pdf.
6. Qun Li et al. Early Transmission Dynamics in Wuhan, China,of Novel Coronavirus–Infected Pneumonia. The new England Journal of Medicine, March 26, 2020.
7. KieshaPrem, Yang Liu, Timothy W Russell, Adam J Kucharski, Rosalind M Eggo, Nicholas Davies. The effect of control strategies to reduce social mixing on outcomes of the COVID-19 epidemic in Wuhan, China: a modelling study www.thelancet.com/public-health Published online March 25, 2020 https://doi.org/10.1016/S2468-2667(20)30073-6.
8. Christian Hubbs. Social Distancing to Slow the Coronavirus: Modeling the flattening of the COVID-19 peaks. Toward data science, Mar, 2020, https://towardsdatascience.com/social-distancing-to-slow-the-coronavirus-768292f04296.
9. Jairo C. O. Quintans, José A. Silva. Model of dynamic epidemic system with numerical simulation in Python. Biomatemática, 28 (2018), 101–114.
10. Kabir, K. M. A., Kuga, K., Tanimoto, J. Analysis of SIR epidemic model with information spreading of awareness. Chaos, Solitons and Fractals 119 (2019) 118–125.
11. Epstein JM, Parker J, Cummings D, Hammond RA (2008) Coupled Contagion Dynamics of Fear and Disease: Mathematical and Computational Explorations. PLoS ONE 3(12): e3955. doi:10.1371/journal.pone.0003955.
12. Jinling Zhou, Yu Yang, Tonghua Zhang. Global stability of a discrete multigroup SIR model with nonlinear incidence rate. Mathematical Methods in the Applied Sciences, Volume 40, Issue 14, 2017.
13. Haitao Song, Shengqiang Liu, Weihua Jiang. Global dynamics of a multistage SIR model with distributed delays and nonlinear incidence rate. Mathematical Methods in the Applied Sciences, Volume 40, Issue 6, 2016.
14. Sergio L. M. Londoño. Estimation of the Basal Reproduction Number in Compartmental Models. Master's Thesis, Statistics Program, UNICAMP, 2014. http://repositorio.unicamp.br/jspui/bitstream/REPOSIP/305840/1/MercadoLondono_SergioLuis_M.pdf.
15. Mehran Sabeti. Discrete epidemic study SIR with age structure and application of pulse and constant vaccination. Doctoral thesis in Mathematics, Universidade Federal de Pernambuco, 2011. https://repositorio.ufpe.br/bitstream/123456789/1321/1/arquivo2722_1.pdf
16. Zaili Zhen, Jingdong Wei, Lixin Tian, Jiangbo Zhou, Wenxia Chen. Wave propagation in a diffusive SIR epidemic model with spatiotemporal delay. Mathematical Methods in the Applied Sciences, Volume 41, Issue 16, 2018.
17. Rejane C. Dorn. Analysis of Dengue Dynamics through the number of reproducibility based on epidemiological data. Doctoral Thesis in Physics, Universidade Federal da Bahia, 2016. https://blog.ufba.br/pgif/files/2017/04/T27-IF-UFBA.pdf

18. WHO-China Joint Missionon Coronavirus Disease 2019. https://www.who.int/docs/default-source/coronaviruse/who-china-joint-mission-on-covid-19-final-report.pdf.